

## MEDICAL PHYSICS ASPECTS OF PARTICLE THERAPY

Oliver Jäkel<sup>1,2,\*</sup>

<sup>1</sup>Heidelberg Ion Beam Therapy Center, Im Neunheimer Feld 450, 69120 Heidelberg, Germany

<sup>2</sup>German Cancer Research Center, Im Neuenheimer Feld 280, 69120 Heidelberg, Germany

**Charged particle beams offer an improved dose conformation to the target volume when compared with photon radiotherapy, with better sparing of normal tissue structures close to the target. In addition, beams of heavier ions exhibit a strong increase of the linear energy transfer in the Bragg peak when compared with the entrance region. These physical and biological properties make ion beams more favourable for radiation therapy of cancer than photon beams. As a consequence, particle therapy with protons and heavy ions has gained increasing interest worldwide. This contribution summarises the physical and biological principles of charged particle therapy with ion beams and highlights some of the developments in the field of beam delivery, the principles of treatment planning and the determination of absorbed dose in ion beams. The clinical experience gathered so far with carbon ion therapy is briefly reviewed.**

### INTRODUCTION TO RADIATION THERAPY

The possibility of concentrating the radiation dose to the tumour while sparing the surrounding normal tissue is called dose conformation. The rationale for the development of conformal radiation therapy techniques is found in radiobiology. The probability of controlling the growth of a tumour increases with the delivered dose. The same is true, however, for the probability of radiation-related side effects in normal tissue. In many clinical cases, the dose that can be delivered to a tumour (and hence the tumour control) is limited by the radiation tolerance of the surrounding normal tissue. It has been observed, however, that the radiation tolerance of many organs is increasing if the irradiated volume of that organ is decreased (the so-called dose-volume effect). Consequently, if the irradiated volume of normal tissue can be minimised by conformal radiation therapy, a higher dose can be delivered to the tumour and thus a better outcome can be achieved without increasing the risk of side effects. This effect is the basis of most developments in the field of radiation therapy in the last decades. The highest degree of dose conformation can currently be achieved with proton and ion beams.

The idea to use heavy charged particles in radiation medicine dates back to 1946 when Robert R. Wilson, a physicist who had worked on developing particle accelerators, proposed the use of protons for cancer therapy<sup>(1)</sup>. Less than 10 y later, in 1954 protons were used to treat cancer patients for the first time in Berkeley and in 1955 also helium ions were used at the same facility<sup>(2)</sup>. In 1977 heavier ions, like neon, silicon and argon were introduced for cancer therapy also at the Lawrence Berkeley Laboratory and many encouraging results (especially

in skull base tumours and paraspinal tumours) were achieved<sup>(3,4)</sup>.

Today, particle therapy with protons and carbon ions has gained increasing interest. Worldwide, there are ~25 therapy units for treating patients with protons within a hospital environment and a total of about 55,000 patients have been treated with protons. There are more than 20 centres under construction or in the planning phase that will start to treat patients within the next 5 y<sup>(2)</sup>.

The availability of heavy ion radiotherapy (RT) is currently limited, as worldwide only three facilities offer carbon ion RT: two hospital-based facilities in Japan (HIMAC/Chiba and HIBMC/Hyogo) and one in Heidelberg, Germany. There is, however, an increasing interest in ion RT, especially in Japan and Europe, where new facilities are being built in Gunma (Japan), Germany<sup>(5)</sup> and Italy<sup>(6)</sup> or are in an advanced planning phase such as in Austria and France.

### INTERACTIONS OF PROTONS AND IONS

#### Energy loss and energy transfer

As the physical and biological properties of proton beams differ significantly from beams of heavier particles, there is a distinction between the two categories ‘proton therapy’, characterised by low linear energy transfer (LET) and ‘heavy-ion therapy’, with high LET properties.

Charged particles passing through tissue slow-down losing energy in atomic interactions. This reduces the energy of the particles, which in turn causes increased energy loss, reaching a maximum at the end of range and causing the maximum dose deposition within the target area. In addition, due to nuclear interactions the number of primary particles is reduced and light fragments are produced.

\*Corresponding author: o.jaekel@dkfz.de

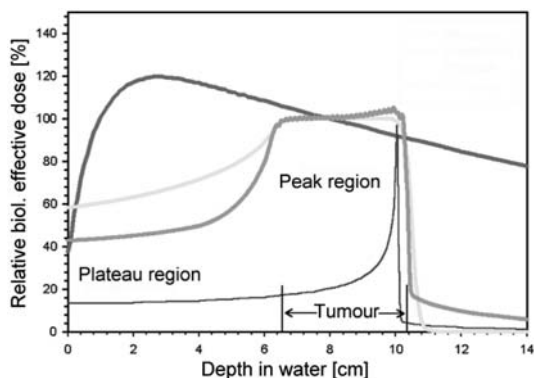


Figure 1. Biologically effective dose, as a function of the penetration depth in water, for MV photon beams (15 MV, red line), a monoenergetic carbon ion Bragg peak ( $220 \text{ MeV u}^{-1}$ , blue line) and spread-out Bragg peaks of protons (120 MeV; yellow line) and carbon ions ( $220 \text{ MeV u}^{-1}$ ; green line). The given numbers are relative units, normalised to dose at an 8-cm depth. For protons a constant RBE of 1.1 is assumed. The RBE for carbon was calculated using the track structure model by Scholz (see text, reproduced from ref.<sup>(29)</sup>).

The primary rationale for RT with heavy charged particles is this sharp increase of dose in a well-defined depth (Bragg peak) and the rapid dose fall-off beyond that maximum (Figure 1).

The electronic stopping power ( $S_{\text{col}}$ ) of heavy charged particles can be calculated to first order using Bethe's equation as follows:

$$S_{\text{col}} = \text{const.} * \rho \frac{Z z^2}{A \beta^2} \left[ \ln \left( \frac{2m_e c^2 \beta^2}{I(1 - \beta^2)} \right) - \beta^2 \right] \quad (1)$$

Here,  $Z$ ,  $A$ ,  $\rho$  and  $I$  are the atomic charge, mass, density and mean ionisation potential of the target material, respectively. The  $z$  and  $\beta$  quantities are the charge and relative velocity (relative to the speed of light) of the projectile, respectively.

From equation (1) it follows that a carbon ion of  $\sim 300 \text{ MeV u}^{-1}$  (which has an approximate range of 16 cm in water) has an energy loss that is roughly a factor of 25 larger than a proton at 150 MeV that has roughly the same range (128 versus  $5.5 \text{ MeV cm}^{-1}$ ).

Monoenergetic Bragg peaks are usually not wide enough to cover most treatment volumes. By superimposing a set of beams with decreasing energies and weights, a 'Spread-out Break Peak' (SOBP) is generated, which delivers the desired dose to the whole treatment volume (Figure 1).

The ratio of Bragg peak dose versus dose in the entrance region is larger for heavy ions than for protons. Due to their larger mass, multiple and

energy straggling becomes negligible for heavy ions when compared with protons. Heavy ions therefore offer an improved dose conformation when compared with photons and proton RT, with better sparing of normal tissue structures close to the target.

For the biological effects of protons and ions, the number and energy of secondary electrons are the most important. The maximum kinetic energy  $W_{\text{max}}$  transferred to a secondary electron by a heavy charged particle can be calculated by simple kinematics as follows:

$$W_{\text{max}} \cong 2m_e c^2 \left( \frac{\beta^2}{1 - \beta^2} \right) \quad (2)$$

Here, the approximation has been made that the electron mass ( $m_e$ ) can be neglected compared with the proton or ion mass. It is immediately clear that the maximum energy from carbon or proton beams at the same range is only about a factor of 2 larger than for protons ( $\beta = 0.26$  for protons versus 0.43 for  $^{12}\text{C}$ , with the energies specified above). The main difference in the secondary electron spectra, thus, is that the number of electrons produced in a carbon beam must be at least an order of magnitude larger than in a proton beam.

Moreover, the average energy of secondary electrons is much smaller than the maximum energy (which is below 1 MeV for  $^{12}\text{C}$  at  $350 \text{ MeV u}^{-1}$ ), since the energy loss distribution follows a Landau distribution that is very asymmetric. The resulting average kinetic energy of a secondary electron for protons and ions is around 1 keV. This means that the large amount of energy, lost by the ions is transferred to a very small volume around the track of the primary ion. This is reflected by the term 'densely ionising particles' and has important consequences for the biological effectiveness of ion beams. Typical particle tracks are shown in Figure 2.

### Angular scattering

Protons and ions undergo multiple scattering just like electrons but with the difference that the average scattering angles are orders of magnitude smaller due to the ballistic properties of protons and ions. The multiple scattering distributions can be accurately described by the theory of Molière and safely approximated by a Gaussian function, allowing straightforward application of the Fermi-Eyges theory.

This results in penumbræ for protons and ions that are comparable or better than high-energy photon beams rather than electron beams. In Figure 3, however, the deterioration of the penumbræ as a function of depth is shown, which leads to

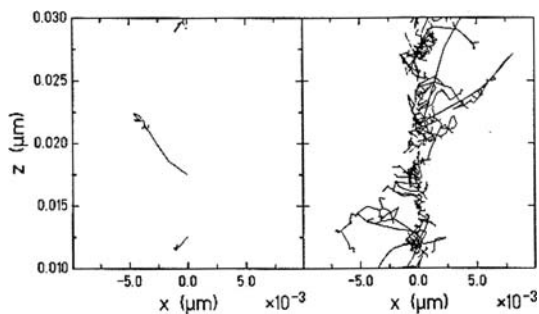


Figure 2. Calculated tracks of secondary electrons produced by a 1-MeV proton (left) or a 1-MeV  $u^{-1}$  carbon ion, which passes at  $x=0$  along the  $z$ -direction (reproduced from ref.<sup>(30)</sup>).

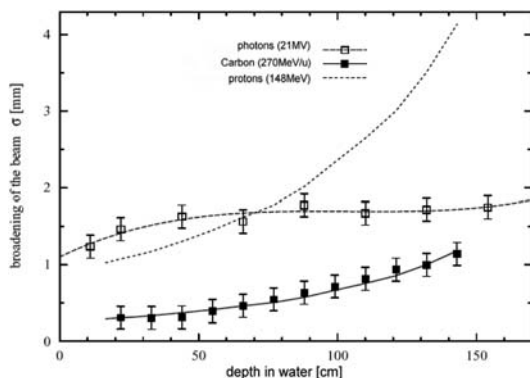


Figure 3. Penumbrae as a function of depth for carbon ions, protons and high-energy photons (reproduced from ref.<sup>(31)</sup>).

a point where proton penumbrae are worse than for photons even if they were sharper at the surface. Heavier ions are favourable from this point of view.

### Nuclear interactions

Protons and ions in the clinical energy range have a substantial probability to undergo a non-elastic nuclear interaction. These reactions basically remove particles from the primary beam and can be treated as an attenuation mechanism. For proton-induced reactions, the unstable nuclei that are the result of the absorption can emit one or more secondary protons, which will contribute to the fluence as a function of depth besides neutrons and gamma rays, as well as a smaller number of heavier fragments and recoils.

For ions, the range of reaction products from the nuclear interactions is wider and, furthermore, the ions themselves can undergo fragmentation as a

result of the interaction with the target nucleus. Target fragmentation is relatively unimportant, since the target fragments typically have very low energies and ranges well below 1 mm. In contrast, the light projectile fragments have a larger penetration depth than the primary particles leading to a fragmentation tail beyond the Bragg peak, as seen in Figure 1. For carbon ions, inelastic nuclear interactions not only lead to attenuation of the primary particle number and build-up of fragments, but also to a halo of light fragments, which are emitted at an angle relative to the trajectory of the primary ions. Due to their lower charge, the dose deposited by this halo is, however, relatively small.

The resulting complex radiation spectrum is of importance for the understanding of the biological effects of ion beams, but also for modelling the response of radiation detectors, like ionisation chambers, thermoluminescence detectors or radiochromic film response. Modelling of these nuclear fragmentation effects is, therefore, an important problem in the application of ion beams in cancer therapy.

## RADIOBIOLOGICAL ASPECTS OF PROTON AND ION BEAMS

### Relative biological effectiveness

In addition to the dose conformation, heavy ions exhibit a strong increase of the LET in the Bragg peak when compared with the entrance region. This increase is due to the track structure as explained above. The radiobiological advantage of high-LET radiation in tumour therapy is well known from neutron therapy. Unlike in RT with neutron beams, in heavy ion RT the high-LET region can be conformed to the tumour. The increasing biological effectiveness of ions with larger charge is shown in Figure 4.

While helium ions are very similar to protons in their biological properties, carbon or neon ions exhibit an increased relative biological effectiveness (RBE) in the Bragg peak when compared with the entrance region. The RBE ratio (Bragg peak versus entrance region) is the highest for carbon ions as in Figure 4. For ions heavier than neon, the RBE in the entrance region is even higher than in the Bragg peak (like for argon).

Another disadvantage of heavy ions for RT is the increase of nuclear fragmentation processes, which leads to a fragment tail in the depth-dose distribution that extends beyond the Bragg peak.

### Oxygen-enhancing ratio and other effects

Besides the larger effect in cell killing, there are some more radiobiological effects that make heavier

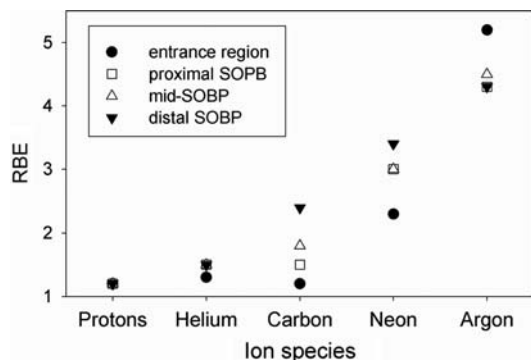


Figure 4. RBE for crypt cells of mice after irradiation with ions in different positions of the spread-out Bragg peak (SOBP). The modulation of the SOBP was 8–10 cm, the initial beam energy was 160, 225, 400, 557 and 570 MeV  $u^{-1}$  for p, He, C, Ne and Ar ions, respectively. Figure reprinted from ref.<sup>(32)</sup>

ions beneficial for tumour therapy. For example, it is known that for low-LET radiation the survival of cells depends critically on the oxygen saturation of tissue. This is due to the production of oxygen radicals in the cell due to radiation. Many solid tumours, which exhibit hypoxic areas, are therefore very resistant to low-LET radiation. For high-LET radiation, it is known that the oxygen saturation of tissue plays only a minor role. High-LET particles should, therefore, be especially useful in the treatment of radio-resistant tumours. There is also a smaller variation in the sensitivity of cells in different parts of the cell cycle when using high-LET radiation instead of low-LET radiation.

### Modelling of RBE

Although the fact that RBE is depending on many different parameters as mentioned above, it was concluded that for proton therapy the magnitude of RBE variation with treatment parameters in clinical situations is only of the order of  $\sim 10$ – $20$ %. The average value at mid-SOBP over all dose levels was shown to be 1.1. At almost all institutions proton therapy is based on the use of a single RBE value (=1.1) which is applied to all proton beam treatments independent of dose/fraction, position in the SOBP, initial beam energy or the particular tissue.

The higher biological effectiveness of high-LET radiation when compared with low-LET radiation can be modelled by so-called track-structure models<sup>(7,8)</sup>. According to these models the basic difference of high- and low-LET radiation, is the high local dose that is deposited close to the primary particle track of a high-LET particle. If one

assumes that the nonlinear relation between cell survival and dose can be applied also for sub-volumes of a cell nucleus (where ‘lethal events’ in the cell nucleus are considered) it becomes clear that the integral effect for the cell nucleus is dependent on the pattern of the local dose distribution: irradiation of small sub-volumes with a high dose is more effective than a homogeneous dose over the whole nucleus (keeping the average dose constant). If assumptions on the local radial dose distributions are made, this can be used to extract the relative biological effectiveness for ion beams from known survival data for cells after low-LET irradiation.

## BEAM PRODUCTION AND DELIVERY

### Cyclotrons versus synchrotrons

One of the basic features of heavy ions is their strongly increased energy loss or LET when compared with protons, which is responsible for their RBE characteristic. Consequently, the ion energy required to treat deep-seated tumours is much higher; while a proton beam of 150 MeV can penetrate 16 cm in water, the same radiological depth is achieved with carbon ions of 3000 MeV or 250 MeV  $u^{-1}$  (energy per nucleon). To accelerate particles to such high energies, synchrotrons are better suited than cyclotrons, which are more common in proton RT. Particle acceleration in synchrotrons is somewhat more complex and maybe more cost intensive than in cyclotrons. Nevertheless, there are also some proton therapy centres based on synchrotrons.

Also ion sources for heavier ions are more difficult to design than for protons, where simple hydrogen gas targets of high purity are available. To inject the ions into a synchrotron ring, they have to be accelerated first in a linear accelerator (Linac) injector to several MeV  $u^{-1}$ . Such a Linac consists of a radio-frequency cavity and a drift tube and has a length of several metres. All these components make ion beam production considerably more costly than proton beams.

Differences also arise as cyclotrons are delivering constant beam intensity, while a synchrotron beam is pulsed. An advantage of the latter is, however, that beam parameters like energy, focus and intensity can be changed from pulse to pulse.

### Beam-line and facility design

The high momentum of ions at therapeutic energies leads to a higher magnetic beam rigidity when compared with protons. The rigidity is defined as the product of the bending radius and the required magnetic field strength. Maximum energies used for ions are around 400 MeV  $u^{-1}$ . At this energy the beam

rigidity is 6.3 Tm when compared with 2.2 Tm for a proton beam of the same range. To achieve a reasonable bending radius, much higher field strengths and thus larger and heavier magnets are necessary for ions. While the weight of a proton gantry is already around 100 tonnes (at a diameter of 10 m), an isocentric gantry for carbon ions has a weight of about 600 tonnes at a diameter of 13 m.

The large size and weight of such a gantry together with the high spatial accuracy required for the beam position at the isocentre is a technical challenge. Instead of flexible beam delivery systems, fixed vertical or inclined beam lines have been realised at the clinical ion facilities in Japan and also in the facilities under construction in Marburg and Kiel. Typically vertical beams or beams with 45° inclination are available together with horizontal beams. Another option to achieve more flexibility is the usage of treatment chairs or rotatable moulds for the patient.

### Active and passive beam delivery

There are two basic methods to shape the beam and to tailor the dose to the target volume, which will be described in the next section.

Passive beam delivery techniques (Figure 5) use double-scattering systems or wobbling magnets in combination with scatterers to produce large particle fields<sup>(9)</sup>. The particle field is then confined to the tumour cross section by individually manufactured collimators or multileaf collimators.

To generate the SOBP, a rotating modulator wheel is inserted into the beam. This device introduces periodically material of varying thickness into the beam that results in a periodical modulation of the range. Alternatively, a static filter of varying thickness may be applied. This so-called ridge-filter uses bar-ridge energy absorbers to produce a homogeneous range modulation over the lateral extension of the treatment field.

Each modulator wheel or ridge filter is connected to a specific SOBP and is selected according to the extension of the tumour in depth. To adjust the SOBP to the distal edge of the tumour, range shifters are used.

Finally, compensators manufactured for the individual field of each patient can be used to adjust the dose distribution to the distal edge of the tumour. As the extension of the SOBP remains constant over the tumour cross section, the dose conformation at the distal edge is connected to high doses in the normal tissue at the proximal edge of the tumour (Figure 5).

Another way of beam delivery is called active beam shaping<sup>(10)</sup>. This system takes advantage of the electric charge of the particles, in order to produce a tightly focused pencil beam that is then

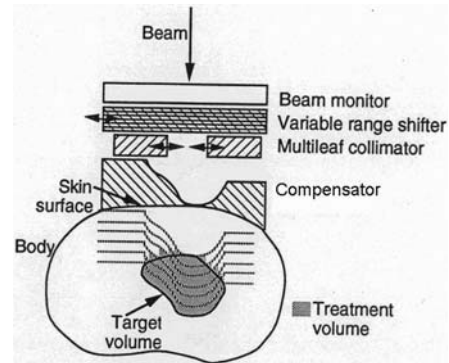


Figure 5. Principle of the passive dose delivery. Shown is the incoming broadened beam that is modulated in depth. The range shifter shifts the SOBP to the desired depth, while collimator and compensator are patient-specific devices. The lines in the body represent the distal dose fall-off that can be shifted in depth with the range shifter (reproduced from ref.<sup>(29)</sup>).

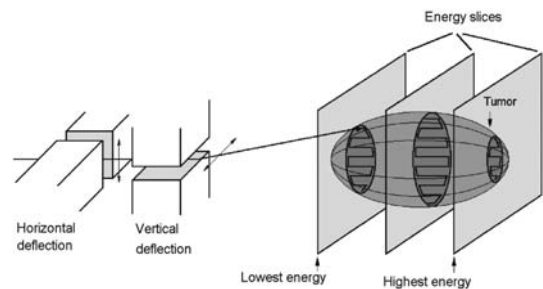


Figure 6. Principle of an active beam delivery: a monoenergetic pencil beam is scanned over the tumour cross section. After one slice is irradiated the energy of the beam extracted from the synchrotron can be switched to the next energy (reprinted from ref.<sup>(29)</sup>).

deflected laterally by two magnetic dipoles to allow a scanning of the beam over the treatment field.

When the beam is produced with a synchrotron, the energy can be switched from pulse to pulse in order to adapt the range of the particles in tissue. This way, a target volume can be scanned in three dimensions and the dose distribution can be tailored to any irregular shape without any passive absorbers or patient-specific devices, like compensators or collimators.

Therefore, the high-dose region can also be conformed to the proximal end of the target volume and the integral dose as well as the non-target volume receiving high-LET radiation is minimised.

Figure 6 shows the principle of the active beam delivery system. There is only one facility (GSI) where beam scanning for carbon ions was applied clinically. The GSI beam delivery system allows for a

3D scanning of arbitrarily shaped volumes with a spatial resolution of 1 mm in all three directions. Typically, a beam width of 3–10 mm full-width half-maximum is scanned over a regular grid of points with typically 2–3 mm spacing. The accelerator energy can be switched from pulse to pulse and the energy can be selected from a library of 252 accelerator energies.

An essential prerequisite for such a beam scanning system is a suitable beam diagnostic system that is capable of monitoring the exact position and intensity of the beam at each beam spot. The monitoring system is connected via a feedback loop to the scanner magnets.

The intensity monitors are calibrated in terms of particle number and are used to switch the beam via the feedback loop to the next scan point if a predefined particle number for a given scan point has been reached.

For detection of the beam position, two additional large area multiwire proportional chambers are installed. They are made up of two wire planes with 112 wires with a spacing of 2 mm. This allows a determination of the beam position with a spatial resolution of better than 0.5 mm at a sampling interval of 150  $\mu$ s. The position data are again fed back to the scanning magnets, so that any deviation of the measured from the desired beam position is immediately corrected for at the next scan point.

## MEDICAL DOSIMETRY

### Ion chamber dosimetry

The determination of absorbed dose to water in all operating ion facilities is currently based on ionisation chamber dosimetry<sup>(9,11,12)</sup>. For this purpose, commercial ionisation chambers (mainly thimble-type chambers) are used, which are calibrated by the secondary standard dosimetry laboratory (SSDL) in a field of Co-60 in terms of absorbed dose to water. This procedure is recommended also in the latest Code of Practice of the International Atomic Energy Agency, the technical report series TRS-398, which is currently the only international guideline for clinical dosimetry of ion beams<sup>(12)</sup>.

According to TRS-398, the absorbed dose to water at an effective point of measurement,  $P_{\text{eff}}$ , of the chamber in an ion beam is determined by

$$D_w(P_{\text{eff}}) = M_{\text{Corr}} N_{D,w,\text{Co-60}} k_Q, \quad (3)$$

where  $M_{\text{Corr}}$  is the dosimeter reading, corrected for changes in air density, incomplete saturation and polarity effects of the chamber. The calibration factor,  $N_{D,w,\text{Co-60}}$ , is given by the manufacturer and  $k_Q$  is a chamber-specific factor that corrects for the

different beam quality of  $^{12}\text{C}$  ions and the calibration beam quality ( $^{60}\text{Co}$ ).

In TRS 398 it is suggested that the  $k_Q$  factor is calculated theoretically as follows:

$$k_Q = \frac{(w_{\text{air}}/e)^{C-12}}{(w_{\text{air}}/e)^{C-60}} \frac{\bar{s}_{w,\text{air}}^{C-12}}{(\bar{L}/\rho)_{w,\text{air}}^{C-60}} \frac{p^{C-12}}{p^{C-60}}, \quad (4)$$

which is a product of the ratios of the  $w$  values, the stopping power ratios of water to air and the chamber-specific perturbation factors for  $^{12}\text{C}$  and  $^{60}\text{Co}$ , respectively. The overall uncertainty of this determination of absorbed dose is stated to be about 3 %.

The calculation of the stopping power ratio has to take into account not only the fluence of primary carbon ions but also the fragments that arise from nuclear interactions and also their energy distribution.

### TLD and film dosimetry

A general problem when using any kind of solid state detectors for ion beam dosimetry, is the effect of quenching of the signal in regions with increased LET. For protons this effect is rather limited and can be corrected for as a function of depth. This way even absolute dose measurements in proton fields can be achieved. For heavier ions the increase in LET is much larger and in addition, due to nuclear fragmentation, the LET varies considerably with depth. It is thus not possible to use either films or TLDs for an absorbed dose determination. Rather they are used for relative measurements or QA purposes<sup>(13)</sup>. An overview of data on film response in proton and ion fields is found in ref.<sup>(14)</sup>.

### Dosimetric verification of dose distributions

In the case of a passive beam delivery technique, the dosimetric verification of a beam of protons or ions is practically identical to conventional (non-IMRT) RT. Here the treatment field can be measured, e.g. by scanning a single ion chamber through the treatment field in a water phantom. If active beam delivery is used, the scanning of ion chambers is not possible and hence multichannel dosimetry systems are needed in order to do efficient dosimetric verification in dynamic beam delivery systems. For this purpose dedicated systems have been developed which allow, for instance, positioning a set of many individual ion chambers in a water phantom and measure doses at various points in the field simultaneously<sup>(15)</sup>. Another possibility is to use multichannel detectors like, for instance, segmented ion chamber arrays (e.g. PTW 729). Although a quantitative dose determination is not possible with film

detectors, they are still important to check geometric parameters of the treatment fields.

### Beam monitor calibration

Like the dosimetric verification, also the calibration of beam monitors for passive systems can be performed in the same way as in conventional RT. This typically includes an individual calibration of each treatment field in terms of monitor units at the reference point. If proper modelling of the beam line is performed, also an empirical calibration for each combination of beam shaping elements can be achieved<sup>(16)</sup>. If a scanning system is used together with an energy selection system, the monitor calibration typically has to be done energy specific, i.e. a calibration of all beam energies has to be done in order to achieve a proper treatment field. In this case, the reference point may be chosen to lie in the entrance region of the individual Bragg peaks, rather than in the SOBP as in the case of passive systems<sup>(17)</sup>.

## THERAPY PLANNING

For the active beam shaping system, a research therapy planning system (TPS) was developed<sup>(18,19)</sup>, which fulfils the needs of the beam scanning system. While a modulator for passive beam shaping is designed to achieve a prescribed homogeneous biologically effective dose for a single field. A 3D scanning system can produce nearly arbitrary shapes of the spread-out Bragg peak (SOBP). The shape of the SOBP therefore has to be optimised separately for every scan point in the irradiation field. The introduction of a 3D scanning system, thus, has some important consequences for the TPS:

- The particle number at every scan point and f.e. energy has to be optimised separately.
- The capability for intensity modulated RT with ions should be taken into account.
- All fields of a treatment plan are applied on the same day to avoid uncertainties in the resulting dose due to set-up errors.
- The dose per fraction should be variable for every patient.
- The scanner control data (energy, beam position, particle number at every beam spot) have to be optimised for each field of every patient.
- An RBE model that allows the calculation of a local RBE at every point in the patient has to be implemented.

### Imaging for TP

While it is a common standard to use CT and MR images to outline the tumour and organs at risk, special attention is put on the CT images used for

treatment planning. CT data are still the only quantitative source of electron density needed to calculate the range of the ions in tissue. To do so, a calibration of X-ray CT numbers to ion ranges relative to water is needed. These relations are usually empirical<sup>(20)</sup> and are only valid for a certain well-defined imaging protocol<sup>(13,20)</sup>.

### Dose calculation

The dose calculation for active beam shaping systems relies on measured data for the depth–dose curves. Instead of the measured depth–dose data for the SOBP resulting from the modulators, data for the single energies are needed. If the applied dose is variable, it is necessary to base the calculation of absorbed dose on absolute particle numbers rather than on relative values. For the calculation of the absorbed dose, the integral data including all fragments are sufficient.

Before the actual dose calculation starts, the target volume is divided into slices of equal radiological depth (Here the same empirical methods of range calculation as for passive systems are used). Each slice then corresponds to the range of ions at certain energy of the accelerator. The scan positions of the raster scanner are then defined as a quadratic grid for each energy. In the last step, the particle number at each scan point is optimised iteratively until a predefined dose at each point is reached.

### Dose optimisation and intensity modulation

The most straightforward optimisation of (biological effective) dose is a technique which may be called single field uniform dose optimisation. In the case of passive systems, this is achieved by an optimisation of the design of the range modulator. In the case of protons a homogeneous absorbed dose throughout the depth modulation is produced. For heavier ions the increase of RBE with LET and thus depth necessitates a decrease of the absorbed dose with depth.

In the case of scanning systems, much more flexibility into the possible optimisation of single field is introduced. The additional degree of freedom of depth–dose modulation enables several additional techniques, like the individual biological modelling of RBE (see below) and the use of intensity modulated particle therapy (IMPT). Due to the additional degree of freedom of the depth dose, IMPT can be achieved by various approaches as follows: an IMRT-like optimisation of dose in 2D (keeping the depth modulation fixed), a 2½D optimisation (with an additional, but fixed depth–dose modulation throughout the field) or a real 3D optimisation of all individual scan spots. The more degrees of freedom are used, the more it becomes important to have

additional dose constraints in order not to produce degenerated solutions of the optimisation process<sup>(21)</sup>.

### Calculation of biological effective dose

To fulfil the demands of an active beam delivery on the TPS concerning the biological effectiveness, a more sophisticated biological model is needed. Such a model was developed, for instance, at GSI<sup>(7,8)</sup>. Its main idea is to transfer known cell survival data for photons to ions, assuming that the difference in biological efficiency arises only from a different pattern of local dose deposition along the primary beam. It is therefore also called the local effect model (LEM).

The model takes into account the different energy deposition patterns of different ions and is, thus, able to model the biological effect resulting from these ions. An important prerequisite for this is, however, the detailed knowledge of the number of fragments produced as well as their energy spectrum. The calculated RBE shows a dependence on the dose level and cell type if the underlying photon survival data for this respective cell type are known.

Another important prerequisite for the LEM model is the knowledge on the particle track structure, i.e. the radial dose distribution around the ion track, as a function of the particle charge and energy.

The LEM allows the optimisation of a prescribed biologically effective dose within the target volume<sup>(18)</sup> using the same iterative optimisation algorithm as for the absorbed dose. At each iteration step, however, the RBE has to be calculated anew, as it is dependent on the particle number (or dose level). Since this includes the knowledge of the complete spectrum of fragments, the optimisation is rather time consuming. Again, it has to be pointed out that the dose dependence of the RBE demands the use of absolute dose values during optimisation.

## CLINICAL ASPECTS

About 55,000 patients have up to now been treated with protons<sup>(2)</sup>. The experience with carbon ions is much more limited: At the NIRS/Chiba, more than 4000 patients have been treated with carbon ions<sup>(22)</sup>. At GSI, almost 450 patients have been treated<sup>(23–26)</sup>. Both, proton and carbon ion RT, enable dose escalation and optimal sparing of surrounding sensitive normal tissue structures.

### Proton indications and clinical experience

The main advantage of protons in comparison with photons is the reduction of the integral dose to healthy tissue outside the planning target volume, which is due to the 'inverse depth–dose profile' (i.e. Bragg peak) of proton beams. Radiation-induced

side effects including the risk for secondary malignancies can thus be reduced. This point is of major importance when children, adolescents and young adults are to be treated. This advantage is especially pronounced in comparison with modern photon IMRT. While photon IMRT achieves almost comparable target coverage and sparing of adjacent normal tissue from the high-dose region of the dose distribution, the volume of normal tissue outside the planning target volume receiving low doses is much larger with IMRT (see ref.<sup>(27)</sup> for a review).

The treatment of paediatric tumours is one of the most important indications for proton therapy as a clear clinical benefit by means of reduced toxicity is assumed. Advantages for proton RT were found for tumours of the head and neck region, the skull base, the orbit, the brain and extra-cranial sites. Proton RT is therefore preferred in children and adolescents whenever available, although clinical phase III trials are lacking.

Besides the treatment of childhood tumours and the treatment of benign skull base tumours and arteriovenous malformations in adolescents and young adults, the effectiveness of proton RT has been proved in large patient series for uveal melanomas, chordomas and low-grade chondrosarcomas of the skull base. In most proton centres, proton therapy is offered to localised non-small cell lung cancer (NSCLC) patients and prostate cancer patients as well.

A clinical phase II trial of proton RT in stage I NSCLC has been carried out at the Loma Linda University Medical Center (LLUMC), USA.

To fully exploit the advantages of high-precision techniques in the treatment of localised lung cancer, movements of the target due to breathing have to be minimised. In the case of a scanned beam, interference effects between the movement of the beam and the internal organ movements may cause significant problems and need special attention. While respiratory gating and image-guided RT are currently being integrated into modern photon RT as well as into proton RT, tracking of the tumour motion with the scanned beam is currently being experimentally investigated and not yet in clinical application.

Eight-year disease-free survival rates obtained with proton RT in localised prostate cancer at the LLUMC, USA, were very similar to the rates obtained with modern photon IMRT, which is not surprising as applied doses are very similar.

Dose escalation with proton RT is investigated in an ongoing trial at the Massachusetts General Hospital in Boston, USA. A randomised clinical trial investigating high-dose proton RT versus high-dose photon IMRT is still needed in order to answer the question whether the physical advantage of proton RT translates into a measurable benefit by means of quality of life.

### Ion beam indications and clinical experience

Since the availability of ion beams is still limited, there is only very little clinical experience with ion beams, especially when ions heavier than helium are considered. In 2009 nearly 5000 patients have been treated worldwide with carbon ions. More than 4000 patients were treated at the Japanese heavy ion facility HIMAC, which has been in operation since 1994.

At HIMAC a number of studies are ongoing using ion RT for the treatment of tumours of the head and neck, prostate, lung, liver as well as sarcomas of soft tissue and bone and uterine carcinomas. A report on the clinical results is found in ref.<sup>(22)</sup>.

The fractionation scheme used is generally 16 fractions in 4 weeks for head and neck tumours as well as for sarcomas of bone and soft tissue. It was significantly shortened for lung cancer (9 fractions in 3 weeks) and liver tumours (12 fractions in 3 weeks) and is being further shortened to 4 fractions in 1 week for both indications. The latest results are from dose escalation studies in lung tumours and soft tissue sarcoma.

At GSI, about 450 patients have been treated with carbon ions between 1997 and 2008. An overview of the results is found in refs<sup>(20–23)</sup>. The majority of patients were treated for skull base tumours. The median dose was 60 Gy (RBE)<sup>1</sup> (20 fractions each 3Gy (RBE)—the quantity Gy (RBE) denotes the RBE weighted dose, or biologically effective dose.). The 5-y overall local control rate was 91%. The observed side effects were only very moderate.

Figure 7 shows an example of a treatment plan for a patient with a chondrosarcoma close to the brain stem treated with carbon ions at GSI. The excellent dose conformation of the 90 % isodose to

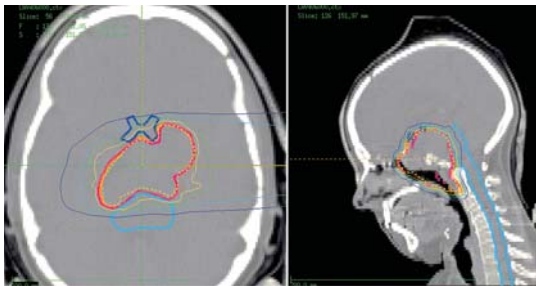


Figure 7. Treatment plan with two fields of carbon ions. Iso-doses of 10, 30, 50, 70 and 90 % of the total dose (60 Gy (RBE)) are shown, respectively. Thick lines indicate target volumes (red), brain stem (light blue), optic and chiasm (dark blue), respectively.

<sup>1</sup>The quantity Gy (RBE) denotes the RBE weighted dose, or biologically effective dose.

the target is clearly demonstrated, although only two horizontal treatment fields were used here. The dose sparing of the relevant organs at risk can also be seen in the dose distribution. Another group of patients was treated at GSI for a malignant salivary gland tumour (adenoid cystic carcinoma) using a combination of photon therapy and a carbon ion boost. The carbon therapy is given only to the macroscopic tumour residual (dose 18 Gy (RBE)), while the photon dose is given to a much larger volume.

An analysis showed that an actuarial local control rate of 75 % at 5 y can be achieved, while in patients treated with photons alone, only 25 % control rate could be achieved<sup>(26)</sup>. Again, severe side effects were observed only in a few patients.

### Hospital-based facilities

Pioneering work in the field of RT with heavy protons and ions was performed at the University of California, Berkeley. The Bevalac provided the scientific and technological basis for many of the current developments in the field of ion RT.

Proton therapy was then established at various physics research centres already in the 1950s, e.g. in Uppsala (Sweden) and Harvard (the USA). The first hospital-based proton facility was opened in 1991 at Loma Linda Medical Center (the USA).

The Heavy Ion Medical Accelerator HIMAC started its clinical operation at Chiba, Japan, in 1994. Until today about 4000 patients have been treated with carbon ions<sup>(22)</sup>. Two synchrotrons deliver carbon ion beams at energies of 290, 350 and 400 MeV u<sup>-1</sup>.

Patients are treated in three different treatment rooms, the first equipped with a vertical beam line, the second a horizontal beam line and the third with a vertical and a horizontal beam line, respectively.

There are currently a number of suppliers that offer turn-key proton RT facilities which are all based on very similar solutions. The most widespread solution by IBA Inc. offers protons that are delivered from a 250-MeV isochronous superconducting cyclotron. The cyclotron has a diameter of 5 m.

The high-energy beam lines deliver the beam to several treatment rooms, equipped with isocentric gantries.

There are currently a number of new ion beam therapy facilities, which have been finalised like in Heidelberg (Germany), are under construction like in Pavia (Italy), Gunma (Japan) or Marburg (Germany) or are in an advanced planning state like in Lyon (France) or Wiener Neustadt (Austria). Most of these facilities offer proton as well as ion beams and are equipped with either a combination of horizontal and vertical fixed beam lines or even

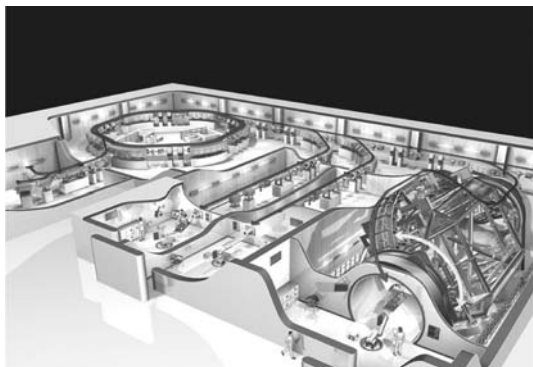


Figure 8. Layout of the Heidelberg Ion Beam Therapy Center. Shown are the two ion sources (left), the LINAC-injectors, the synchrotron and two fixed-beam treatment rooms and the isocentric gantry (reproduced from ref.<sup>(28)</sup>).

gantry solutions (like in Heidelberg). As an example the layout of the new Heidelberg ion beam therapy facility (HIT) at the University Hospital Heidelberg is shown in Figure 8.

A combination of a radiofrequency quadrupole (RFQ) and a linac is used as an injector for the synchrotron. In the RFQ-Linac ions are accelerated from  $7 \text{ keV u}^{-1}$  to  $8 \text{ MeV m}^{-1}$ . This injector delivers beam pulses of varying length and intensities. The synchrotron has a diameter of around 22 m and is based on a ring of six normal conducting dipole magnets. A slow extraction method extracts beam pulses of variable lengths and energy, which are then transported towards the three treatment rooms.

Two of the treatment rooms are equipped with a horizontal fixed beam and a third is equipped with an isocentric gantry. All beam lines are designed for active energy variation of the synchrotron and beam scanning is available in all treatment rooms. For experimental purposes there is a dedicated area. The treatment rooms are equipped with robotic patient positioning and imaging systems.

## OUTLOOK

In the last decade, at 30 centres worldwide valuable clinical experience has been gained in charged particle therapy. Together with the development of new technologies especially for beam application and treatment planning there will certainly be a broader implementation of ions in clinical settings that allow for an optimal exploitation of the physical and biological potential of protons and heavy ions.

Especially in Europe a number of hospital-based facilities are planned that will allow to treat patients with proton as well as carbon ions. The first facility of this kind is the Heidelberg Ion Therapy facility at the University of Heidelberg. It features two ion

sources for rapid switching between proton and ion RT, the possibility to also investigate other ion species, like helium, oxygen or nitrogen, a variable energy extraction from the synchrotron and beam scanning in all treatment rooms. Moreover, the first isocentric ion gantry is installed here.

Many new proton-ion facilities are under construction. This will facilitate the conduction of large-scale clinical trials, which are necessary to answer the open questions<sup>(28)</sup>.

## FUNDING

This work was partially funded by the Helmholtz Foundation of Research Centers (HGF) and the German Science Foundation (DFG).

## REFERENCES

1. Wilson, R. R. *Radiological use of fast protons*. *Radiology* **47**, 487–491 (1946).
2. Sisterson, J. (ed.) *Particle Newsletter 36*, Harvard (2005).
3. Castro, J. R. *et al.* *Experience in charged particle irradiation of tumors of the skull base 1977–1992*. *Int. J. Radiat. Oncol. Biol. Phys.* **29**, 647–655 (1994).
4. Castro, J. R. *Clinical programs: a review of past and existing hadron protocols*. In: *Advances in Hadron Therapy*. Amaldi, U., Larrson, B. and Lemoigne, Y. Eds. (Amsterdam, Netherlands: Elsevier Science) pp. 79–94 (1997).
5. Heeg, P., Eickhoff, H. and Haberer, T. *Conception of heavy ion beam therapy at Heidelberg University (HICAT)*. *Z. Med. Phys.* **14**, 17–24 (2004).
6. Amaldi, U. *CNAO: The Italian centre for light-ion therapy*. *Radiother. Oncol.* **73**(Suppl 2), S191–S201 (2004).
7. Scholz, M. and Kraft, G. *Track structure and the calculation of biological effects of heavy charged particles*. *Adv. Space Res.* **18**, 5–14 (1996).
8. Scholz, M., Kellerer, A. M., Kraft-Weyrather, W. and Kraft, G. *Computation of cell survival in heavy ion beams for therapy – the model and its approximation*. *Rad. Environ. Biophys.* **36**, 59–66 (1997).
9. Kanai, T., Endo, M. and Minohara, S. *et al.* *Biophysical characteristics of HIMAC clinical irradiation system for heavy-ion radiation therapy*. *Int. J. Radiat. Oncol. Biol. Phys.* **44**, 201–210 (1999).
10. Haberer, T., Becher, W., Schardt, D. and Kraft, G. *Magnetic scanning system for heavy ion therapy*. *Nucl. Instrum. Meth.* **A330**, 296–305 (1993).
11. Hartmann, G. H., Jäkel, O., Heeg, P., Karger, C. P. and Krießbach, A. *Determination of water absorbed dose in a carbon ion beam using thimble ionization chambers*. *Phys. Med. Biol.* **44**, 1193–1206 (1999).
12. International Atomic Energy Agency (Ed.). *Absorbed dose determination in external beam radiotherapy*. Technical Report Series No 398 (Vienna: IAEA) (2000).
13. Jäkel, O., Hartmann, G. H., Karger, C. P. and Heeg, P. *Quality assurance for a treatment planning system in*

- scanned ion beam therapy. *Med. Phys.* **27**, 1588–1600 (2000).
14. Martisikova, M., Ackermann, B., Klemm, S. and Jäkel, O. *Use of Gafchromics EBT films in heavy ion therapy.* *Nucl. Inst. Meth. A* **591**, 171–173 (2008).
  15. Karger, C. P., Jäkel, O., Hartmann, G. H. and Heeg, P. *A system for three-dimensional dosimetric verification of treatment plans in intensity-modulated radiotherapy with heavy ions.* *Med. Phys.* **26**, 2125–2132 (1999).
  16. Kooy, H. M., Schaefer, M., Rosenthal, S. and Bortfeld, T. *Monitor unit calculations for range-modulated spread-out Bragg peak fields.* *Phys. Med. Biol.* **48**, 2797–2808 (2003).
  17. Jäkel, O., Hartmann, G. H., Karger, C. P., Heeg, P. and Vatnitsky, S. *A calibration procedure for beam monitors in a scanned beam of heavy charged particles.* *Med. Phys.* **31**, 1009–1013 (2004).
  18. Krämer, M., Jäkel, O., Haberer, T., Kraft, G., Schardt, D. and Weber, U. *Treatment planning for heavy ion radiotherapy: physical beam model and dose optimization.* *Phys. Med. Biol.* **45**, 3299–3317 (2000).
  19. Jäkel, O., Krämer, M., Karger, C. P. and Debus, J. *Treatment planning for heavy ion radio-therapy: clinical implementation and application.* *Phys. Med. Biol.* **46**, 1101–1116 (2001).
  20. Jäkel, O., Jacob, C., Schardt, D., Karger, C. P. and Hartmann, G. H. *Relation between carbon ions ranges and X-ray CT numbers.* *Med. Phys.* **28**(4), 701–703 (2001).
  21. Lomax, A. J. *Intensity modulated proton therapy and its sensitivity to treatment uncertainties I: the potential effects of calculational uncertainties.* *Phys. Med. Biol.* **53**, 1027–1042 (2008).
  22. Tsujii, H., Mizoe, J. E. and Kamada, T. *et al. Clinical results of carbon ion radiotherapy at NIRS.* *J. Rad. Res.* **48**(Suppl A), A1–A13 (2007).
  23. Schulz-Ertner, D., Nikoghosyan, A. and Hof, A. *et al. Carbon ion radiotherapy of skull base chondrosarcomas.* *Int. J. Radiat. Oncol. Biol. Phys.* **67**, 171–177 (2007).
  24. Schulz-Ertner, D., Morath, A. and Nikoghosyan, A. *et al. Effectiveness of carbon ion radiotherapy in the treatment of skull base chordomas.* *Int. J. Radiat. Oncol. Biol. Phys.* **68**, 449–457 (2007).
  25. Schulz-Ertner, D., Nikoghosyan, A. and Didingler, B. *et al. Therapy strategies for locally advanced adenoid cystic carcinomas using modern radiation therapy techniques.* *Cancer* **104**, 338–344 (2004).
  26. Schulz-Ertner, D., Haberer, T. and Scholz, M. *et al. Acute radiation-induced toxicity of heavy ion radiotherapy delivered with intensity modulated pencil beam scanning in patients with base of skull tumors.* *Radiother. Oncol.* **64**, 189–195 (2002).
  27. Schulz-Ertner, D., Jäkel, O. and Schlegel, W. *Radiation therapy with heavy charged particles.* *Sem. Radiat. Oncol.* **16**(4), 249–259 (2006).
  28. Jäkel, O., Karger, C. P. and Debus, J. *The future of heavy ion radiotherapy.* *Med. Phys.* **35**, 5653–5663 (2008).
  29. Jäkel, O. *Hadrontherapy: radiotherapy using fast ion beams.* In: *Ion Beam Science: Solved and Unsolved Problems.* Sigmund, P. Ed. (Copenhagen) pp. 37–57 (2006).
  30. Amaldi, U. and Kraft, G. *Recent applications of synchrotrons in cancer therapy with carbon ions.* *Europhys. News* **36**, 114–118 (2005).
  31. Kraft, G. *Tumor therapy with heavy charged particles,* *Prog. Part. Nucl. Phys.* **45**, S473–S544 (2000).
  32. Jäkel, O. *Heavy ion radiotherapy.* In: *New Technologies in Radiation Oncology.* Schlegel, W., Bortfeld, T. and Grosu, A. L. Eds. (Heidelberg: Springer) pp. 365–378 (2006).